RSC Advances

PAPER

View Article Online
View Journal | View Issue

Cite this: *RSC Adv.*, 2021, **11**, 22761

An adherent drug depot for retinal ganglion cell protection and regeneration in rat traumatic optic neuropathy models†

Lingli Li,‡[ab] Fen Deng,‡[ac] Haijun Qiu,‡[ab] Yao Li,[ab] Zan Gong,[ab] Lei Wang,[de] Jingjie Wang,[ab] Wencan Wu*[ab] and Kaihui Nan*[ab]

Traumatic optic neuropathy (TON) describes an injury to the optic nerve following either blunt or penetrating trauma, and remains an important cause of vision loss. No generalized treatment of TON has been established so far to restore the injured optic nerve. We developed an adherent drug-encapsulated bi-layered depot (DBP) as a dual drug vehicle for local treatment to protect the residual retinal ganglion cells (RGCs) and regenerate axons following optic nerve damage. The inner layer of the depot was prepared by co-electrospinning poly(D,L-lactide-*co*-glycolide acid) (PLGA: 75 : 25) and collagen (COL) with the hydrophobic corticosteroid triamcinolone acetonide (TA) loaded. The outer layer was made of PLGA and the hydrophilic neuroprotective agent Fasudil (FA). The DBP showed suitable morphology, hydrophilicity and mechanical properties, and slowly released TA and FA *in vitro* by undergoing time-dependent degradation and swelling. All depots showed good biocompatibility with L929 mouse fibroblasts, and DBP was helpful in maintaining the morphology of RGCs *in vitro*. In addition, direct implantation of DBP at the injured optic nerve in a rat model mitigated inflammation and the death of RGCs, and increased the expression of nerve growth-related protein GAP-43. Therefore, DBP maybe a promising local therapy against TON in future.

Received 9th December 2020
Accepted 21st June 2021

DOI: 10.1039/d0ra10362d

rsc.li/rsc-advances

Introduction

Traumatic optic neuropathy (TON), an acute injury to the optic nerve that can lead to loss of vision, is the result of blunt trauma to the head or face, when suffering traffic accidents, military activity or natural disasters.[1] The incidence rate of TON is approximately 1 per million, and usually seen in young adults.[2,3] It is often categorized into direct and indirect types according to the mode of injury. Direct TON is the result of the mechanical disruption of the optic nerve due to direct physical stress, such as penetration of a foreign body, displaced fracture fragment or optic canal fracture. Indirect TON results from trauma to the head or face, wherein the force of impact does not directly affect the optic nerve.[4,5] Nevertheless, both direct and indirect TON involve a damaged optic nerve, which are often difficult to distinguish. Primary injury to the optic nerve causes immediate damage from either direct or indirect TON. The subsequent inflammation upregulates apoptosis factors, and the concomitant swelling of optic nerve tissue within the limited bony canal compresses the capillaries to form ischemic damage, resulting in secondary injury due to retinal ganglion cell (RGC) death.[4] Since the optic nerve cannot regenerate in adults following primary injury under current clinical technology,[6] lots of attentions has been paid to prevention secondary injury and protection the residual RGCs.

No evidence-based therapy has been established hitherto for treating TON.[7] High-dose corticosteroid regimen, surgical decompression or their combination can minimize secondary TON by decreasing inflammation and edema, and alleviate ischemic damage.[5,8–11] In addition, long term administration with high doses of corticosteroids results in mild to life threatening complications, including glaucoma, cataracts, skin irritations, weight gain, recurrent infections, osteoporosis, diabetes mellitus and neurologic/psychiatric changes in almost 90% of the patients.[12,13] On the other hand, T. Sugiyama *et al.* found that topical application of ROCK inhibitor may suppress the impairment of optic nerve function and morphology.[14] Besides, localized drug delivery, in which different drugs are

[a]*School of Ophthalmology & Optometry, Affiliated Eye Hospital, Wenzhou Medical University, Zhejiang Province, P. R. China. E-mail: nankh@163.com*

[b]*State Key Laboratory of Ophthalmology, Optometry and Visual Science, Zhejiang Province, P. R. China*

[c]*The 2nd Affiliated Hospital and Yuying Children's Hospital, Wenzhou Medical University, Zhejiang Province, P. R. China*

[d]*University of Chinese Academy of Sciences Wenzhou Institute, Zhejiang Province, P. R. China*

[e]*Engineering Research Center of Clinical Functional Materials and Diagnosis & Treatment Devices of Zhejiang Province, Wenzhou Institute of Biomaterials and Engineering, Wenzhou, Zhejiang 325027, China*

† Electronic supplementary information (ESI) available. See DOI: 10.1039/d0ra10362d

‡ These authors contributed equally to this work.

encapsulated, have been developed to deliver therapeutic agents directly to target site with decreased systemic toxicity, higher drug stability, bioactivity and bioavailability.[15,16] With the development of tissue engineering and materials technology, electrospinning has demonstrated promising results in local drug delivery to treat nerve injury. This method can facilitate different drug encapsulation and transportation through a number of mechanisms.[17]

Several bioactive agents, such as growth factors,[18] neuroprotective factors[6,19] and stem cells,[20] have shown encouraging therapeutic effects in animal models of TON but only a few have been translated clinically. Fasudil, a specific inhibitor of Rho-associated protein kinase (ROCK), has been used to treat cerebral ischemia after subarachnoid hemorrhage in many countries.[21] It can increase cerebral blood flow after stroke by lowering vasoconstriction,[22] and its active metabolite hydroxyfasudil improves cognitive defects in Parkinson's disease[23] and traumatic brain damage.[24] Furthermore, fasudil also induces neurite outgrowth and inhibits inflammation after nerve injury in animal models.[25,26] Systemic administration of fasudil in rabbits can restore blood flow to the optic nerve, and inhibited apoptosis of RGCs.[14,27] On the other hand, intravitreal triamcinolone acetonide (TA) injection has been reported to decrease inflammatory and improve final visual acuity of disc swelling in nonarteritic anterior ischemic optic neuropathy cases.[28] TA has also been proved to be effective in stabilization the blood-retinal barrier and prevent osmotic swelling of Müller cells in diabetic retina.[29,30] Previous studies have suggested the combinations of therapeutic agents could display positive effect for nerve system injury.[31,32] Therefore, we presumed that combination of fasudil with TA can potentially regulate secondary injury, protect RGCs and stimulate axonal regeneration after TON.

Currently, nasal endoscopy becomes mainstream of TON treatment,[33,34] and the very limited space around the optic nerve prevents subsequent suture. Therefore, we designed a self-adherent patch for localized delivery of the corticosteroid triamcinolone acetonide (TA) and fasudil to mitigate secondary TON injury. Poly(lactic-*co*-glycolic acid) (PLGA) and collagen (COL) has been adopted to construct the biocompatible depot since they are FDA approved biomaterials, and have been widely applied in drug delivery and tissue regeneration in nervous system.[35] The inner layer was made from PLGA and collagen because TA is a very hydrophobic drug. PLGA/COL layer can adsorb more liquid to speed up TA release. The outer layer was made from PLGA because FA is a hydrophilic drug. The release of FA would be slowed down by encapsulation of PLGA. Considering the significantly different water solubility of FA and TA, the bilayer drug reservoir was constructed to regulate the release rate of drugs. In addition, the hydrophilic surface of inner layer allowed spontaneous adhesion to the tissue without requiring any suture.

To the best of our knowledge, this is the first study to report simultaneous encapsulation of two drugs in a bilayer electrospun depot for TON treatment at injured site. Our hypothesis was that applying DBP directly to the injured optic nerve would release the drugs locally to protect the residue RGC, promote RGC survival and axonal regeneration.

Experimental and methods

Materials and animals

Poly(lactic acid–glycolic acid) (PLGA, 75 : 25, MW = 50 000) was purchased from Jinan Daigang Biomaterials Co. Ltd (Shandong, China). Collagen from bovine achilles tendon (COL, CAS No. 9007-34-5), hexafluoroisopropanol (HFIP), triton-100, triamcinolone acetonide (TA), and dimethyl sulfoxide (DMSO) were obtained from Sigma-Aldrich China (Shanghai, China). Fasudil dihydrochloride (FA) was bought from J&K Scientific Ltd (Beijing, China). DMEM medium, neurobasal-A medium, fetal bovine serum, B27, ciliary neurotropic factor (CNTF), recombinant human brain-derived neurotrophic factor (BDNF), penicillin–streptomycin solution, Hanks' balanced salt solution (HBSS), phosphate buffered saline (PBS) were provided by Thermo-Fisher Scientific China (Shanghai, China). Cell-counting Kit 8 (CCK8), Live and Dead Cell Assay kit, mouse anti-RBPMS antibody, mouse anti-GAP-43 antibody, and goat anti-mouse IgG H&L (HRP) were purchased from Abcam China (Shanghai, China). Acetonitrile (analytical grade), methanol (analytical grade) and triethylamine (analytical grade) were obtained from Merck China (Shanghai, China). RGCs were provided by Procell Life Science & Technology Co. Ltd (Wuhan, China).

Sprague Dawley® rats (Charles River, China), obtained from Laboratory Animal Center, Wenzhou Medical University, were housed under standard conditions with free access to food and water. All animal experiments were in compliance with guidelines for the care and use of laboratory animals and were approved by the Animal Management and Ethics Committee, Wenzhou Medical University.

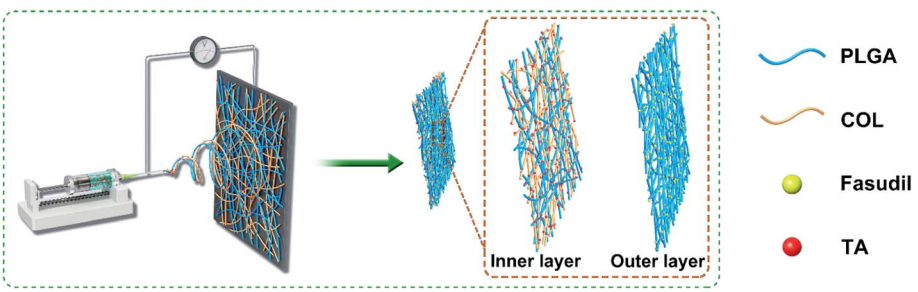

Fig. 1 Schematic illustration of DBP fabrication.

Fabrication of drug-encapsulated bi-layered depots

The drug-encapsulated bi-layered depots were synthesized by electrospinning (as shown in Fig. 1). Briefly, 0.7 g PLGA and 0.037 g fasudil dihydrochloride (FA) were dissolved overnight in 5 ml HFIP with constant stirring to form a uniform spinning solution for the outer layer. In addition, 0.525 g PLGA, 0.175 g Col and 0.037 g TA were mixed in 5 ml HFIP and similarly agitated overnight to obtain a homogenous solution for the inner layer. The formulations for different depots were listed out in Table 1. The solutions were passed through a 23-gauge blunt needle at the constant feeding rate of 0.1 mm min^{-1} with a syringe pump; 15 kV voltage was applied to the needle tip and −2 kV to the receiving end. Fibers were collected by a rotating steel cylinder (D = 100 mm) with a distance of 15 cm and the receiving area was pre-defined (ΠDL, where L = 100 mm) by limiting the walking span of injector. The outer layer was formed by depositing PLGA-FA onto the cylinder for about 7 h at 1000 rpm, and the inner layer was prepared with the corresponding solution using identical parameters. Drug-loaded bilayer depots (DBP) were obtained by isolating 10 cm-wide bands from the receiver, and kept in a vacuum oven for 3 days to remove residual solvent. PLGA, PLGA/COL, PLGA-FA and PLGA/COL-TA films were also prepared as controls. All scaffolds were sterilized by gamma irradiation at 10 kGy.[36]

Characterization of drug-encapsulated bi-layered depots

To observe the surface morphology of the depots, samples (n = 3/group) were cut into 5 × 5 mm^2 pieces and sputter-coated with Pd/Au and both sides were imaged under a FE-SEM (Hitachi SU8010, Japan). Four random images were taken for each sample, and the mean diameter of the fibers was calculated using Image J software. The mechanical strength of the depots was evaluated with an Instron Tensile Tester (Instron 5543A, USA) at room temperature with a humidity of 60%. The load cell was set as 2.5 N and displacement was 10 mm min^{-1}. The samples were cut to 10 cm × 0.5 cm pieces and the gauge length was set to 10 mm. The thickness of samples was measured with a digital micrometre. At least five specimens were measured per group. The surface hydrophilicity was measured by water contact angle analysis (n = 5 per group; DataPhysics, Germany). Samples were first cut into rectangular pieces with the size of 1 cm × 5 cm and placed horizontally on the testing platform. 5 μl of distilled water was carefully dropped onto the pieces and the contact angles were measured. To determine the biodegradability of the bilayer membrane, at least 5 samples were cut to 20 mm × 10 mm pieces, weighed, and immersed in PBS for 1, 3, 5, 7 and 10 days, and 2, 3 and 4 weeks at 37 °C. The soaked samples were weighed, and the loss in weight (%) was calculated as $(M_i - M_d)/M_i \times 100$, which M_i represents for the initial dry weight and M_d for dry weight after degradation.

In vitro drug release behavior

The membranes were cut into pieces weighing 18 mg each (5/group) and incubated in 2.5 ml PBS (pH = 7.4) with constant shaking at 120 rpm for varying durations at 37 °C. At each time point, 2 ml of the medium was collected and replaced with the same volume of fresh PBS. The amount of FA and TA in the medium were analyzed by Ultra Performance Liquid Chromatography (UPLC, Shimadzu, Japan). As for TA detection, the mobile phase was a mixture of acetonitrile/water (40 : 60, v/v) with a flow rate of 0.4 ml min^{-1}. A C18 column (Shim-pack XR-ODS III column 2.2 μm, 2.0 mm × 150 mm) was used where TA was detected at 240 nm (30 °C). As for FA analysis, the mobile phase was a combination of triethylamine/methanol (65 : 35, v/v) with a flow rate of 0.2 ml min^{-1}. The identical column was used and FA was tested at 275 nm (25 °C). The cumulative percentage of the drugs released were calculated and presented as mean ± standard deviation.

In vitro cytotoxicity

L929 mouse fibroblasts (ATCC, USA) were cultured in DMEM supplemented with 10% FBS and incubated at 37 °C with 5% CO_2. When cell confluency reached 80%, the cells were digested and seeded into 96-well plates. After 24 h, the medium was discarded and replaced with PBS (blank), fresh medium (negative control), PLGA extract, PLGA/COL extract and DBP extract. The extracts were prepared by protocol of ISO-10993. On day1, 2 and 3, 10 μl of CCK-8 reagent was added to each well and the plate was incubated at 37 °C for 2 h. Then the absorbance was detected using a microplate reader at a wavelength of 450 nm.

The cytotoxicity of DBP against RGCs was evaluated using a live/dead assay. Primary RGCs (CP-R122) from Sprague-Dawley (SD) rats were purchased from Procell Life Science and Technology Co. Ltd, Wuhan, China. RGCs were cultured in Neurobasal-A medium supplemented with 10% FBS, 2% B-27, 5 μg ml^{-1} insulin, 50 ng ml^{-1} BDNF, 10 ng ml^{-1} CNTF and 1%

Table 1 Fabrication parameters of different electrospun depots

	Contents of components (wt%)			
Sample name	PLGA content	Collagen content	TA content	FA content
PLGA	100			
PLGA/COL	75	25		
PLGA-FA	95		5	
PLGA/COL-TA	71.25	23.75		5
DBP	67.5	22.5	5	5

penicillin/streptomycin. The cells were incubated in a humidified environment at 37 °C in 5% CO_2, and the medium was changed every other day. The RGCs were harvested after 72 h, and seeded into the lower chambers of a 24-well transwell plate at a density of 10^6 per well. After 24 h incubation, the medium was replaced with fresh medium, and pre-sterilized depots were placed into the upper chambers. Live/dead cell staining were performed on day 1, 3 and 5 using suitable kits as per the instructions.

Establishment of TON model and therapeutic regimen

In this study, all animal care and use were performed according to the international regulations for the care and use of laboratory animals as approved by the Chinese government (GB14925-2010). A total of 36 adult female Sprague Dawley (SD) rats weighing ~200 g were randomly divided into injury group, FA-intraperitoneal group (10 mg kg^{-1}, 15 mg per ml per day), TA-intravitreal group (5 μl, 40 mg ml^{-1}), PLGA-FA (2 mm × 10 mm), PLGA/COL-TA (2 mm × 10 mm) and DBP (2 mm × 10 mm) groups. The TON model was established as previously described.[18,37] Briefly, the animals were anesthetized with isoflurane (2.5%, 0.8 l $min_{O_2}^{-1}$) and placed in a stereotaxic frame with a gas anesthesia mask to maintain sedation. The body temperature was maintained with an electric blanket. The area around the lateral corner of the eye was depilated and sterilized with iodophors, and the eye was irrigated with normal saline. A 5 mm incision was made on the skin around the lateral obit with scissors to expose part of the optic nerve. A pressure-constant artery clamp (pressure = 100 g) was then used to crush the optic nerve for 10 seconds, approximately 2 mm behind the eye globe. The respective patches were cut into 2 × 10 mm^2 pieces, and implanted into the injured site using microforceps with inner layer as adherent side. FA was injected intraperitoneally, while TA was administered *via* the intravitreous route. After surgery, all animals were returned to their cages and observed at predetermined time points.

Analyzing of RGC survival

The SD rats were euthanized 3, 7 and 14 days after the respective treatments, and their eyeballs were fixed in 4% paraformaldehyde for 1 h. The retinas were carefully isolated under microscope and flat-mounted on a 6-well TCP. After rinsing thrice with PBS, the tissues were blocked with 0.1% BSA in PBS containing 1% Triton X-100 for 4 h. The retinas were then incubated overnight with polyclonal rabbit anti-RBPMS antibody (1 : 200) at 4 °C, rinsed 5 times with PBS, and incubated with goat anti-rabbit IgG H&L secondary antibody (1 : 200) in a rotation shaker at 37 °C for 4 h. After rinsing thrice with PBS, the stained retinas were mounted onto slides and number-coded. 18 peripheral and 18 central images were captured, the positively stained RGCs were counted using Image J 6.0, and the number of RGCs per mm^2 were calculated. Six eyes from each group were analysed for each time point.

Quantification of axonal growth

The extent of RGC axon growth was assessed by GAP-43 immunostaining of the longitudinal sections of the optic nerve. Briefly, 3 μm-thick sagittal retinal sections were cut through the optic nerve head, deparaffinized in xylene, and rehydrated through an ethanol gradient (100%, 95%, 85%, 75%). The sections were blocked with 5% BSA in PBS for 20 min, washed and incubated overnight with primary rabbit anti-GAP-43 (1 : 200) at 4 °C. After incubating with goat anti-rabbit IgG (1 : 200) at 37 °C for 30 min, the sections were stained with DAB substrate kit to show brown color. The area and integrated optic density were measured for 9 regions of interest, randomly

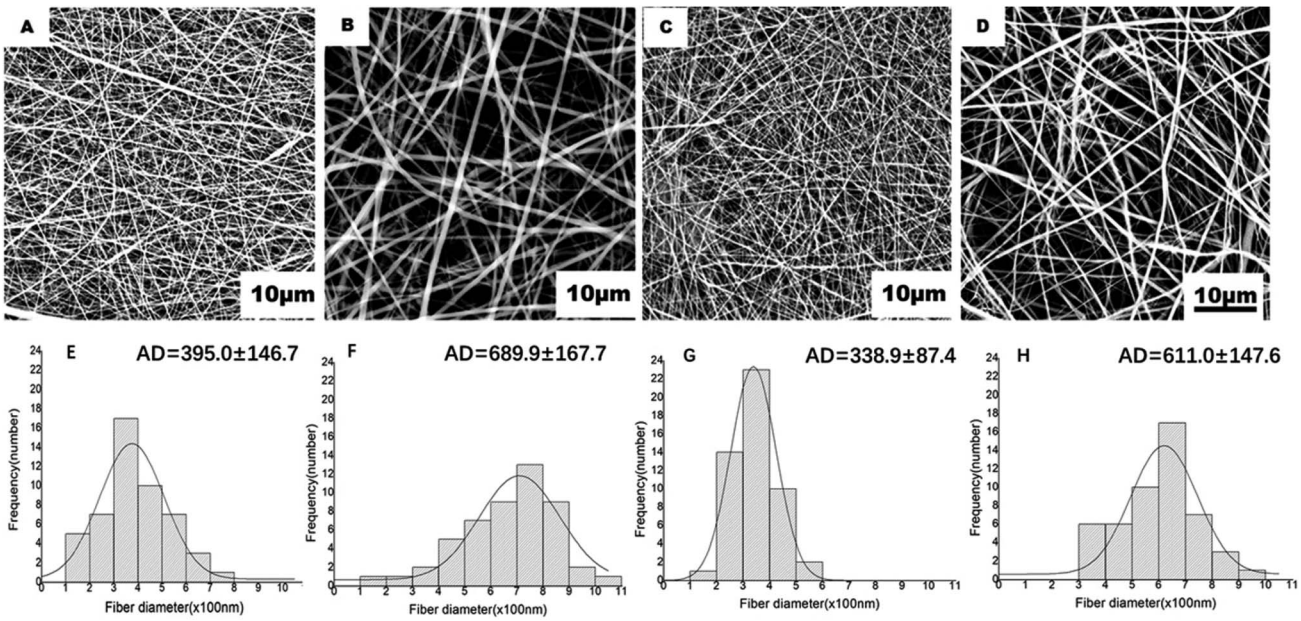

Fig. 2 The surface morphology of electrospun depots. Representative SEM images of outer layer (A), inner layer (B) of DBP, PLGA-FA (C), PLGA/COL-TA (D) and their diameter distribution: outer layer (E), inner layer (F) of DBP, PLGA-FA (G), PLGA/COL-TA(H).

distributed along the optic nerve. The mean optic intensity was calculated as follows: mean pixel intensity = integrated optic density/area.

Histological examination of optic nerve

Enucleation was carried out to examine the pathological change of the optic nerve. Optic nerve slices (5 μm thick) were fixed in 4% paraformaldehyde, embedded in paraffin, and cut into serial sections. The latter were dehydrated through an ethanol gradient (100%, 95%, 85%, 75%), stained with hematoxylin for 5 min, differentiated in 1% (v/v) hydrochloric acid alcohol for 3 s, rinsed with water and 1% aqueous ammonia for 5 s and stained with eosin for 3 min. The stained sections were then dehydrated with an alcohol gradient, cleared with xylene, mounted with neutral gum, dried and observed under a light microscope.

Statistical analysis

The data was expressed as the mean ± SD, and compared by one-way analysis of variance (ANOVA) as appropriate. $P < 0.05$ were considered statistically significant. SPSS 19.0 software was used for all statistical analysis.

Results

DBP is mechanically and biophysically suitable as a drug delivery system

DBPs with an inner PLGA/COL-TA layer and outer PLGA-FA layer were successfully fabricated by electrospinning. As shown in the SEM images in Fig. 2, the depots exhibited similar morphology of electrospun nanofibers to reported research.[38,39] PLGA and PLGA/COL fibers were continuous and well dispersed in a random manner, both layers were highly porous with interconnected fibers. All of the nanofiber diameter distributed in accordance with normal distribution (ESI†). It can be found in the inner layer, nanofibers became thicker with the addition of collagen. The spinnability of these polymer solutions were also greatly reduced with increased drug loading.

The surface hydrophilicity of DBP layers was determined by measuring the water contact angle. A contact angle less than 90° is favorable for wetting, while materials with angles greater than 90° cannot be easily wetted. As shown in Fig. 3A–F, the water contact angle decreased with increasing collagen content in the matrix. Furthermore, encapsulation of FA in PLGA, and of TA in PLGA/Col did not affect the hydrophilicity of the respective depot. Since water was readily absorbed by the porous structure of the electrospun materials, the contact angle also decreased with time.

Although optic nerve is not a load-bearing tissue, it is still required that the DBP has the requisite mechanical properties to support the surgery for TON. As shown in Fig. 3G, the elastic modulus of DBP is 46.04 ± 38.54 MPa, compared to 16.19 ± 1.98 MPa and 90.44 ± 19.94 MPa for PLGA-FA and PLGA/COL-TA respectively, and exceeds the requirement for optic nerve. Furthermore, addition of collagen increased the elastic modulus compared to PLGA-FA, and elastic modulus of DBP are closed to mean value of PLGA-FA and PLGA/COL-TA.

As shown in Fig. 3H, blank DBP, PLGA and PLGA/COL films degraded in a time-dependent manner. DBP lost 30% of the initial weight in the first week of exposure to PBS, and its residual weight was 53% after 60 days. PLGA/COL showed faster degradation rates compared to DBP at the same time points, while PLGA degraded over a period of months.

DBP allows sustained release of encapsulated drugs

As shown in Fig. 4, both FA and TA showed an initial burst in the first 24 hours, followed by a more sustained release. We surmised that the drugs present on the surface were released

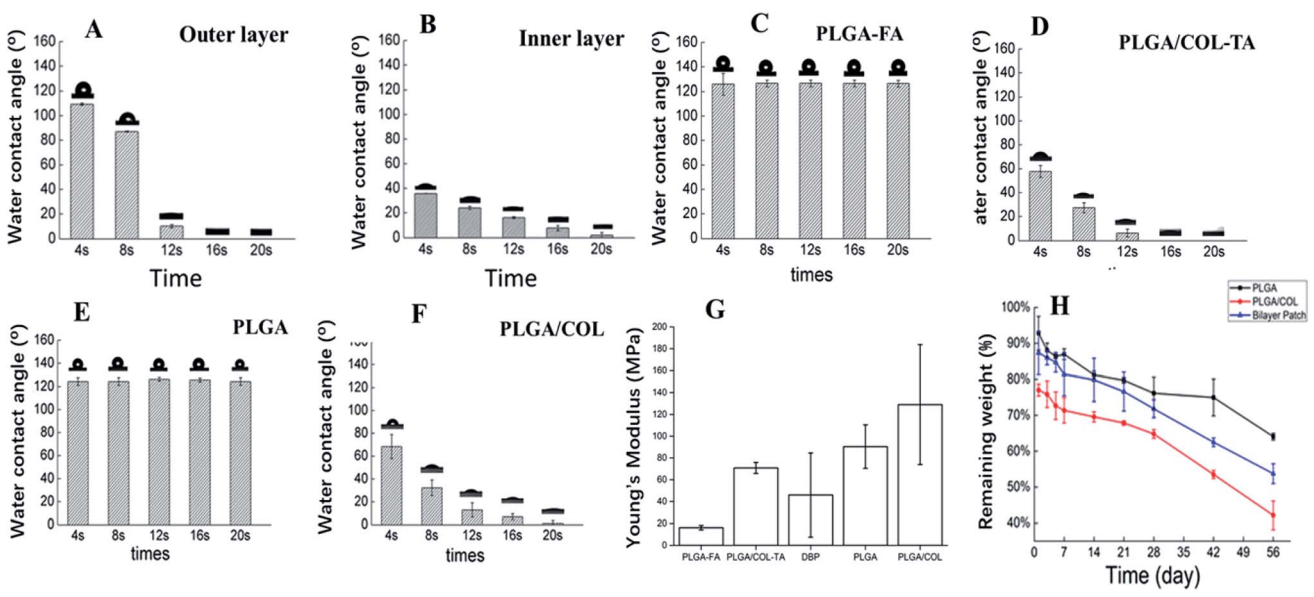

Fig. 3 Characterization of electrspun depots ($n = 5$). (A–F) Water contact angles of outer layer, inner layer, PLGA-FA, PLGA/COL-TA, blank PLGA and PLGA/COL; (G) Young's modulus; (H) *in vitro* biodegradability of blank depots.

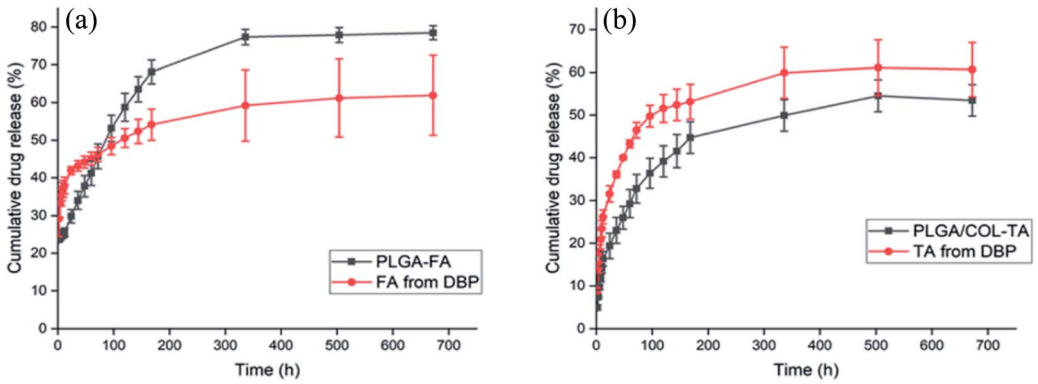

Fig. 4 *In vitro* drug release profiles of different depots: (A) FA, (B) TA.

immediately once DBP was immersed in the buffer, resulting in the initial spike. The residual drugs encapsulated in the matrix then diffused into medium due to the slow degradation of DBP and gradual swelling. In addition, the cumulative percentage of FA released from DBP were 60%, 62% and 69% after 1 day, 3 days and 4 weeks respectively, while TA was released at a much slower rate of 41%, 46% and 61% on the same time points. This is likely due to different water solubility between FA and TA.

DBP exhibited excellent *in vitro* biocompatibility and maintained RGC viability and morphology *in vitro*

The potential cytotoxicity of the blank and drug-loaded nanofibers was tested *in vitro* using L929 mouse fibroblasts and RGCs. As shown in Fig. 5A, regarding to control group, all the blank electrospun membrane did not display toxicity towards L929 cells. RGCs were incubated in 24-well transwell plate with DBP by indirect method. After 1, 3, 5 days, RGCs were stained with Live/Dead Viability Kit. As demonstrated in Fig. 5B, no obvious cytotoxic effect was observed when RGCs were co-cultured with materials for 5 days, conversely, DBP was found to support RGC survival. It can be observed that, the RGCs cultured with DBP displayed typical neuronal morphology with long, extended neurites, whereas the control cells lost the axons after 3 days of culture and became polygonal by day 5.

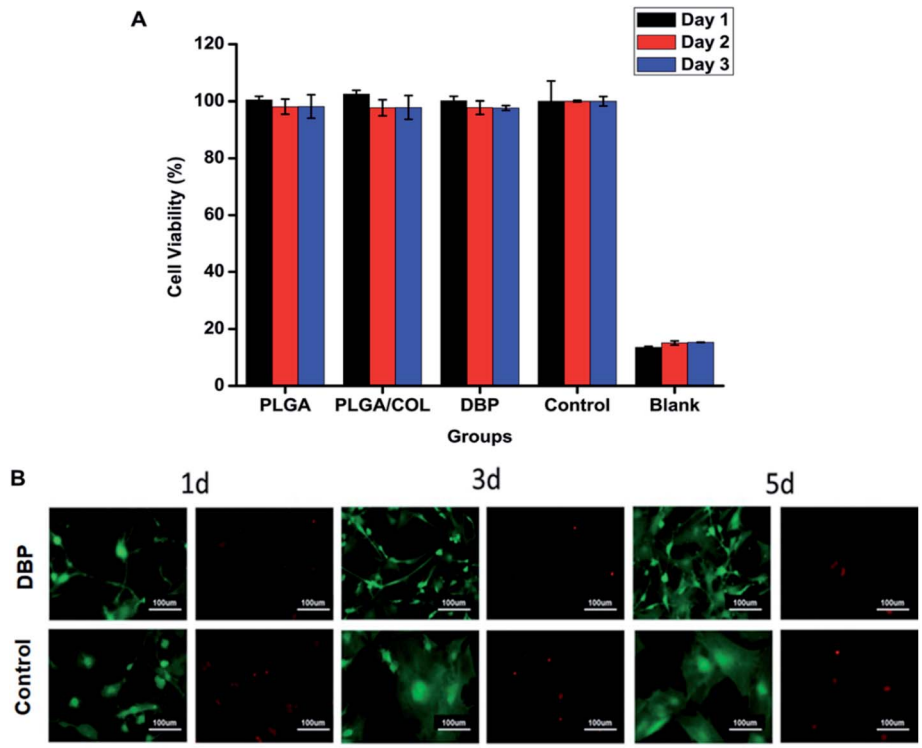

Fig. 5 The biocompatibility of DBP with mouse L929 fibroblasts and RGC cells. (A) L929 cells. CCK-8 analysis showed that no significant toxicity was observed in exacts of blank electrospun membranes over 3 days. (B) RGC cells. Fluorescent images of live/dead assay displayed that DBP was biocompatible with RGC cells.

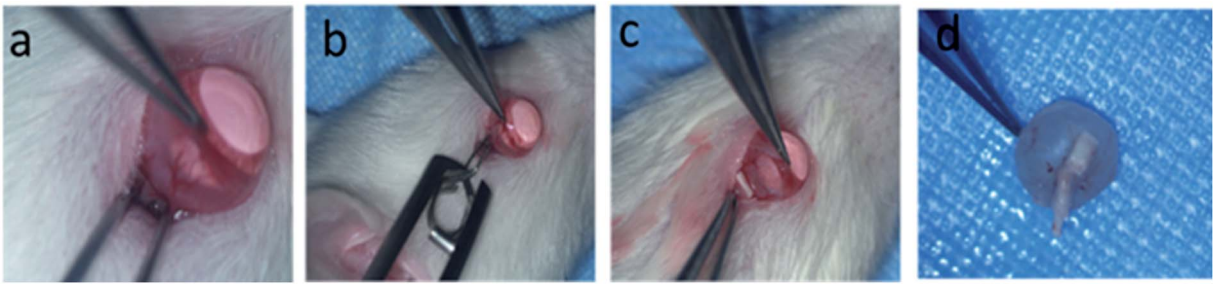

Fig. 6 Establishment of TON in SD rats and depot implantation.

DBP self-adheres to the optical tissues and promotes RGC survival post-TON

To further assess the therapeutic effect of DBP on RGC survival and regeneration following injury to the optic nerve, DBP, PLGA-FA and PLGA/COL-TA depots were implanted into the injured site in SD rats (Fig. 6). DBP and PLGA/COL-TA self-adhered to the surface of the lesion without the need of any suturing or bio-adhesive agents, and remained intact during the observation period. In contrast, the PLGA-FA depot shrank to some extent in the sterilization process and was not tightly

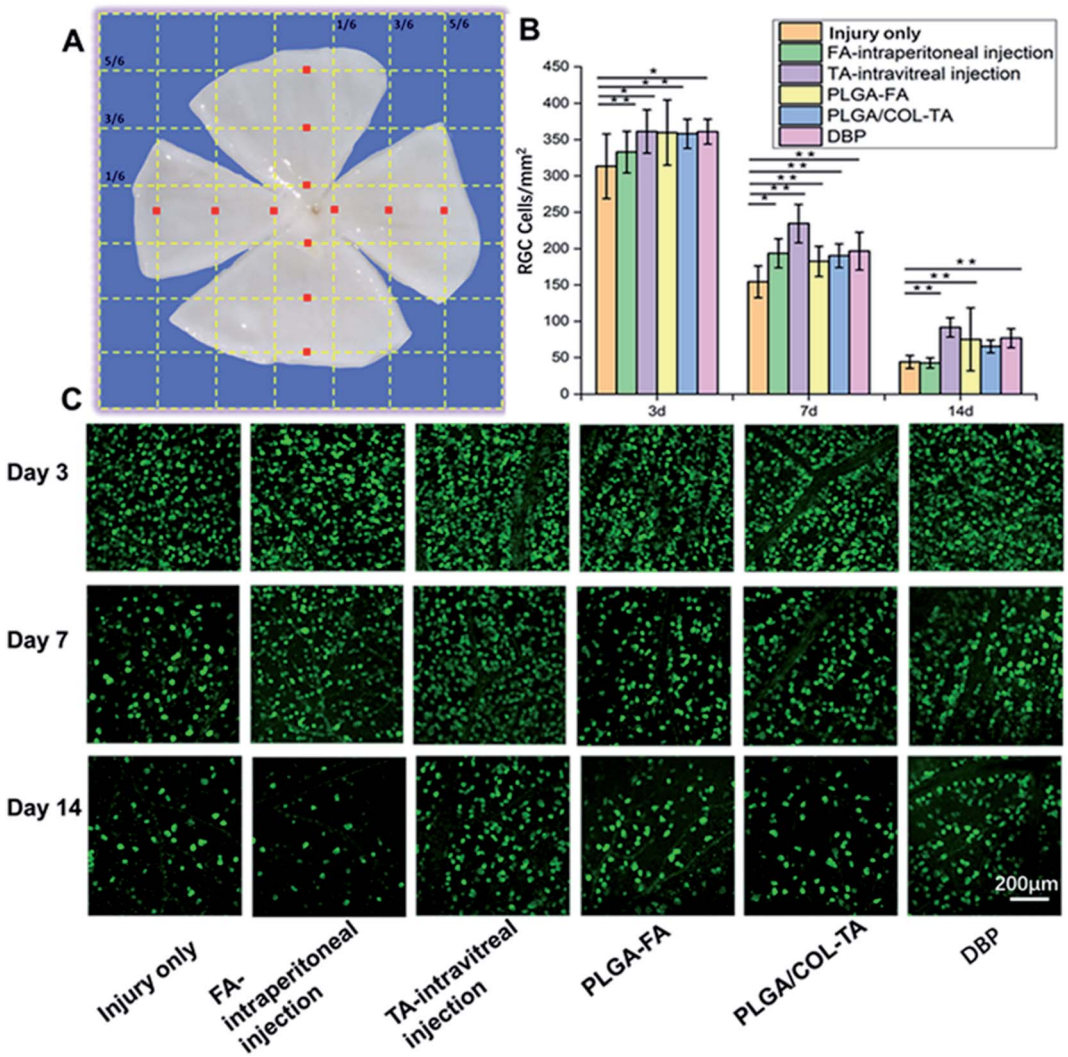

Fig. 7 (A) Micro-image of dissected retinal tissue; (B) quantitation of RGC survival in each group at day 3, 7 and 14; (C) representative images of retinal sections stained with anti-RBPMS antibody on days 3, 7 and 14 post-TON, and the corresponding number of surviving RGCs (*$P < 0.05$, **$P < 0.01$).

affixed to the tissue. DBP was completely wrapped by the connective tissue by 2 weeks. In addition, no irritation or inflammation was observed in the surrounding area, indicating that DBP and its metabolites were compatible with the tissues.

The effect of DBP on the survival of RGCs was determined by analyzing the expression of RBPMS

Optic nerve injury resulted in a gradual decrease in the number of RGCs. As shown in Fig. 7, the percentage of surviving RGCs on days 3, 7 and 14 were least in injury only group, and 37–40% survival rate seen on day 7, which is consistent with previous studies.[17,40] Intravitreal injection of TA and DBP displayed significantly higher RGCs surviving rate on day 7 and 14, and showed better therapeutic effect compared to PLGA-FA, PLGA/COL-TA and intraperitoneal FA. Interestingly, the survival rate of RGCs in FA-intraperitoneal treated animals declined to similar level to injury only group on day 14.

DBP mitigated secondary TON injury by promoting RGC axonal regeneration

Since TON also impairs the axonal structure of the optic nerve, we next determined whether DBP mitigated pathological changes. As shown in Fig. 8, the healthy optic nerve fibers were arrayed closely and parallel to each other, and the glial cells were evenly distributed in the matrix. Direct injury to the optic nerve resulted in edema within 3 days, and progressed to distortion, fracture and loss of nerve fibers in a time-dependent manner, resulting in numerous cavities. In addition, infiltration of inflammatory cells and formation of hyperplastic glial scar prevented the RGC axons from re-growing. All treatment modalities markedly alleviated the pathological changes, and reduced infiltration of inflammatory cells into the crushed site. However, PLGA/COL-TA and TA-intravitreal groups exhibited less structural disorder compared to PLGA-FA and FA-intraperitoneal groups, and DBP groups kept the most structural regularity compared to other 5 groups.

The regenerative ability of DBP was determined by analyzing the expression of GAP-43, a marker of axonal regeneration during nerve growth and repair,[41,42] in the affected axons. GAP-43 is upregulated during the re-growth of optical axons in a temporal manner that is species specific. In the SD rats for example, the damaged optic nerve is regenerated within the first week after damage. As shown in Fig. 9, the GAP-43 staining intensity was significantly higher in the optical axons of animals treated with FA-intraperitoneal injection, PLGA-FA or DBP compared to the injury only PLGA/COL-TA and TA-intravitreal injection groups on day 7 post-implantation ($p < 0.05$). In addition, GAP-43 expression was similar in all three FA-containing groups, while the injury and TA only containing groups were closed to each other. After 14 days, GAP-43 expression decreased slightly in the DBP, PLGA-FA and FA intraperitoneal injection groups, and was not significantly affected in the others, although the DBP and PLGA-FA groups still showed the highest expression levels.

Discussion

There are many barriers, *e.g.* blood–brain barrier, blood–ocular barriers, cornea–aqueous barriers and intrinsic structure, present challenges in drug delivery to the injured optic nerve lesion. Maintaining stability and extending the drug release period is another problem to solve. Delivery a drug depot to target site by nasal microscopy seems a good method to elude many physiological barriers and maintain long-term therapeutic drug levels. In our study, an adherent drug co-encapsulation bi-layered depot was engineered as vehicles for different drugs and facilitate the local delivery of compounds to lesion areas and wrap the optic nerve bundles without any further treatment.

The DBP was made of nonwoven electrospun PLGA and PLGA/COL fibers; PLGA outer layer and PLGA/COL inner layer were combined together to load different drugs and make the depot adherent. The porous structure showed in Fig. 2 is essential for implantable materials, which can facilitate cellular activities, nutrient transportation and drug delivery,[43] and means the surface texture of the bilayer depots is suitable for cell adhesion, migration and drug release. Due to the unique anatomical location of the optic nerve, it is desirable to develop an adherent and biodegradable drug delivery system to adhere to tissues spontaneously. The micronanofibers prepared by electrospinning cause great contact with tissue's surface due to

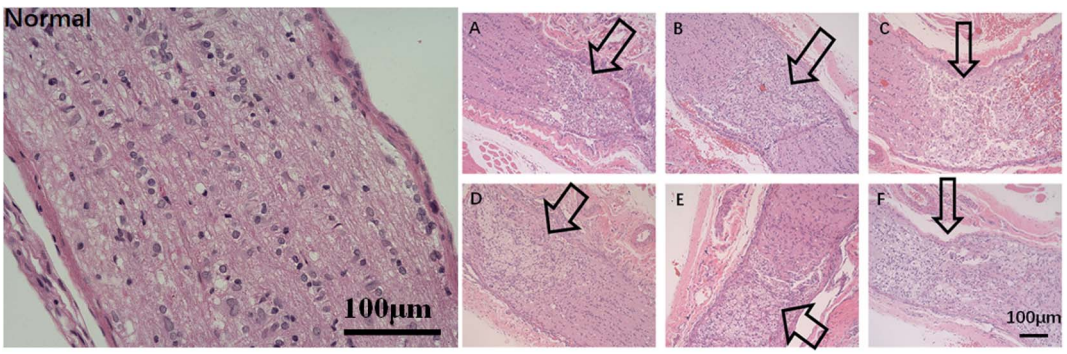

Fig. 8 Representative images of optic nerve sections stained with HE showing pathological changes in the indicated groups after 14 days. (A) Injury only, (B) FA-intraperitoneal injection, (C) TA-intravitreal injection, (D) PLGA-FA, (E) PLGA/COL-TA, (F) DBP.

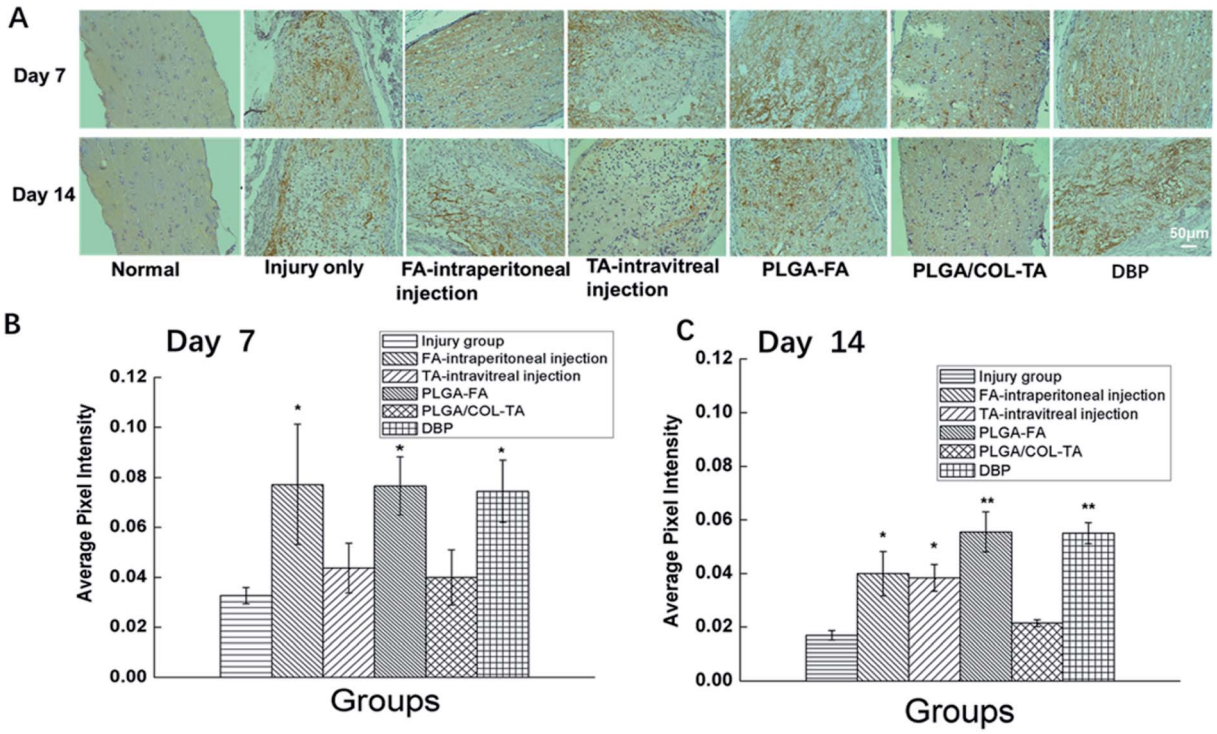

Fig. 9 Immunostaining of RGCs using anti-GAP-43 antibody. (A) Representative images of the longitudinal sections of optic nerve stained with anti-GAP-43 antibody on days 7 and 14 post-TON; (B) quantification of the mean density of optic nerve injured site in each group after 7 days; (C) quantification of the mean density of optic nerve injured site in each group after 14 days (*$P < 0.05$, **$P < 0.01$).

high surface-to-volume ratio.[44] The presence of collagen in the inner layer of DBP enhanced its hydrophilicity and the adhesion of the depot to the tissue surface *via* interaction between collagen and the surface protein of nerve tissue (Fig. 3A–F).[44,45] Thus, the hydrophilic inner surface of DBP not only makes it a suitable carrier for TA, but also creates a self-adherent depot for the tissues. Besides, addition of collagen can accelerate the biodegradation of PLGA, thus making the DBPs applicable for long-term drug delivery (Fig. 2H). Furthermore, the drug kinetics were similar for DBP, PLGA-FA and PLGA/COL-TA, indicating that collagen did not significantly affect drug release from the polymer matrix. FA and TA can be simultaneously loaded into DBP, and delivered *in situ* at different rates (Fig. 4). The localized and sustained delivery of TA and FA can replace frequent systemic administration and synchronize to play their therapeutic roles.

Application of systemic and intravitreal steroids have shown promising outcomes in reducing disc edema and recovering patients' visual outcome, the median time for the complete resolution of swelling was 6.8 weeks, but with potential safety risk.[46] FA not only reduce inflammation to ameliorate patent's visual acuity, but also regulate blood flow to the ischemic optic nerve head to protect damaged axons.[47,48] Similar to other differentiated cells of the mammalian central nervous system, RGCs do not proliferate under common circumstances.[49] *In vitro* cell viability tests showed that sustained release of FA and TA from DBP was effective in keeping them viable and maintaining their typical morphology for longer period than control group (Fig. 5). The results of animal study indicated that not only TA and FA can help more RGCs to maintain viability after trauma but also proved localized rather than systemic administration of drugs can effectively protect RGCs (Fig. 7). Intravitreally-injected TA, PLGA-FA, PLGA/COL-TA and DBP acted as drug depots near RGCs or its axons, and slowly released the drug to alleviate TON-induced apoptosis of RGCs, and increase the surviving RGCs numbers even after two weeks. In contrast, free FA exerted short-term neuroprotective effects but was cleared too rapidly when administered systematically. To sum it up, the increased drug retention within the DBP, PLGA/COL-TA and PLGA-FA depots, and in the vitreous fluid ensures localized drug delivery to the injured site prior to systemic circulation in neuroprotection of RGCs.

FA can promote the regeneration of RGCs axons, but is rapidly metabolized within 2 weeks when administered systematically. Intravitreal and depot mediated delivery of TA also exhibited some regenerative effects, although not as high as FA containing group. Sustained release of TA or FA from vitreous body or different depots mitigated the inflammatory response and secondary damage caused by TON, protected the RGC axons and reduced glial scarring, which is essential for axonal regeneration (Fig. 9). The therapeutic effect of DBP was optimal, the mechanism may lie in that TA and FA work in sync and suppress local edema and increase blood flow to the injured optic nerve, thus creating a conducive microenvironment for RGC axonal regrowth post-TON.

Conclusion

In this work, we developed bilayer depot of electrospun nanofibers for localized delivery of FA and TA to the injured optic nerve to regulate inflammatory and protect RGCs cells from secondary TON. The DBP had the requisite physical and mechanical properties, good biodegradability and excellent biocompatibility to the RGCs, and released TA and FA in a sustainable manner. DBP also can adhere spontaneously to the injured optic nerve site *in vivo*. According to the results, DBP can resolves part of the injury state, *e.g.* delayed RGC loss, promoted RGC survival and axonal growth. In conclusion, the study suggested that localized drug delivery maybe a promising therapeutic strategy in treatment of TON.

Conflicts of interest

There are no conflicts to declare.

Acknowledgements

This work has been partly supported by National Key R&D Plan (2016YFC1101200) and National Natural Science Foundation of China (31600795 and 31570959), the Project of State Key Laboratory of Ophthalmology, Optometry and Visual Science, Wenzhou Medical University (4241319001G), Zhejiang Provincial Natural Science Foundation of China (LGF18C100002), Health Commission of Zhejiang Province (2020KY655), and S&T Program of Wenzhou (Y20190137), Engineering Research Center of Clinical Functional Materials and Diagnosis & Treatment Devices of Zhejiang Province (WIUCASK20004). The authors would like to thank Dr Yikui Zhang (Wenzhou Medical University) and Changcan Shi (University of Chinese Academy of Sciences, Wenzhou Institute) for kindly providing help and useful suggestions on material preparations and animal study respectively.

References

1 S. Ahmad, N. Fatteh, N. M. El-Sherbiny, M. Naime, A. S. Ibrahim, A. M. El-Sherbini, S. A. El-Shafey, S. Khan, S. Fulzele, J. Gonzales and G. I. Liou, Potential role of A2A adenosine receptor in traumatic optic neuropathy, *J. Neuroimmunol.*, 2013, **264**, 54–64.

2 V. Lee, R. L. Ford, W. Xing, C. Bunce and B. Foot, Surveillance of traumatic optic neuropathy in the UK, *Eye*, 2010, **24**, 240–250.

3 R. L. Ford, V. Lee, W. Xing and C. Bunce, A 2-year prospective surveillance of pediatric traumatic optic neuropathy in the United Kingdom, *Journal of American Association for Pediatric Ophthalmology and Strabimus*, 2012, **16**, 413–417.

4 B. C. Chaon and M. S. Lee, Is there treatment for traumatic optic neuropathy?, *Curr. Opin. Ophthalmol.*, 2015, **26**, 445–449.

5 L. Stunkel and G. P. Van Stavern, Steriod Treatment of Optic Neuropathies, *Asia Pacific Academy of Ophthalmoloty*, 2018, **7**, 218–228.

6 V. Sengottuvel, M. Leibinger, M. Pfreimer, A. Andreadaki and D. Fischer, Taxol Facilitates Axon Regeneration in the Mature CNS, *J. Neurosci.*, 2011, **31**, 268–2699.

7 B. C. Tse, G. Dvoriantchikova, W. Tao, R. A. Gallo, J. Y. Lee, S. Pappas, R. Brambilla, D. Ivanov, D. T. Tse and D. Pelaez, Tumor Necrosis Factor Inhibition in the Acute Management of Traumatic Optic Neuropathy, *Invest. Ophthalmol. Visual Sci.*, 2018, **59**, 2905–2912.

8 H. J. Oh, D. G. Yeo and S. C. Hwang, Surgical Treatment for Traumatic Optic Neuropathy, *Korean J. Neurotrauma*, 2018, **14**, 55–60.

9 K. D. Steinsapir and R. A. Goldberg, Traumatic Optic Neuropathy: An Evolving Understanding, *Am. J. Ophthalmol.*, 2011, **151**, 928–933.

10 T. Ropposch, B. Steger, C. Meço, M. Emesz, H. Reitsamer, G. Rasp and G. Moser, The effect of steroids in combination with optic nerve decompression surgery in traumatic optic neuropathy, *Laryngoscope*, 2013, **123**, 1082–1086.

11 W. G. Yang, C. T. Chen, P. K. Tsay, V. Glenda, Y. J. Tsai and Y. R. Chen, Outcome for traumatic optic neuropathy-surgical *versus* nonsurgical treatment, *Ann. Plast. Surg.*, 2004, **52**, 36–42.

12 J. R. Curtis, A. O. Westfall, J. Allison, J. W. Bijlsma, A. Freeman, V. George, S. H. Kovac, C. M. Spettell and K. G. Saag, Population-based assessment of adverse events associated with long-term glucocorticoid use, *Arthritis Rheuma*, 2006, **55**, 420–426.

13 M. Ciriaco, P. Ventrice, G. Russo, M. Scicchitano, G. Mazzitello, F. Sciccitano and E. Russo, Corticosteroid-related central nervous system side effect, *J. Pharmacol. Pharmacother.*, 2013, **4**, S94–S98.

14 T. Sugiyama, M. Shibata, S. Kajiura, T. Okuno, M. Tonari, H. Oku and T. Ikeda, Effects of Fasudil, a Rho-Associated Protein Kinase Inhibitor, on Optic Nerve Head Blood Flow in Rabbits, *Invest. Ophthalmol. Visual Sci.*, 2011, **52**, 64–69.

15 S. D. Putney and P. A. Burke, Improving protein therapeutics with sustained-release formulations, *Nat. Biotechnol.*, 1998, **16**, 153–157.

16 Y. Kitamura, G. Bikbova, T. Baba, S. Yamamoto and T. Oshitari, In vivo effects of single or combined topical neuroprotective and regenerative agents on degeneration of retinal ganglion cells in rat optic nerve crush model, *Sci. Rep.*, 2019, **9**, DOI: 10.1038/s41598-018-36473-2.

17 A. Donsante, J. Xue, K. M. Poth, N. S. Hardcastle, B. Diniz, D. M. O'Connor, Y. Xia and N. M. Boulis, Controlling the Release of Neurotrophin-3 and Chondroitinase ABC Enhances the Efficacy of Nerve Guidance Conduits, *Adv. Healthcare Mater.*, 2020, **9**(14), DOI: 10.1002/adhm.202000200.

18 M. R. Laughter, J. R. Bardill, D. A. Ammar, B. Pena, D. J. Calkins and D. Park, Injectable Neurotrophic Factor Delivery System Supporting Retinal Ganglion Cell Survival and Regeneration Following Optic Nerve Crush, *ACS Biomater. Sci. Eng.*, 2018, **4**, 3373–3383.

19 G. A. Grinblat, R. S. Khan, K. Dine, H. Wessel, L. Brown and K. S. Shindler, RGC Neuroprotection Following Optic Nerve

Trauma Mediated by Intranasal Delivery of Amnion Cell Secretome, *Invest. Ophthalmol. Visual Sci.*, 2018, **59**, 2470–2477.

20 K. Flachsbarth, K. Kruszewski, J. Gila, W. Jankowiak, K. Riecken, L. Wagenfeld, G. Richard, B. Fehse and U. Bartsch, Neural stem cell-based intraocular administration of ciliary neurotrophic factor attenuates the loss of axotomized ganglion cells in adult mice, *Invest. Ophthalmol. Visual Sci.*, 2014, **55**, 7029–7039.

21 K. Nagata, Y. Kondoh, Y. Satoh, Y. Watahiki, E. Yokoyama, H. Yuma, Y. Hirata, F. Shishido, J. Hatazawa and I. Kanno, Effects of fasudil hydrochloride on cerebral blood flow in patients with chronic cerebral infraction, *Clin. Neuropharmacol.*, 1993, **16**, 501–510.

22 H. K. Shin, S. Salomone, E. M. Potts, S. W. Lee, E. Millican, K. Noma, P. L. Huang, D. A. Boas, J. K. Liao, M. A. Moskowitz and C. Ayata, Rho-kinase inhibition acutely augments blood flow in focal cerebral ischemia *via* endothelial mechanisms, *J. Cerebr. Blood. Flow. Metab.*, 2007, **27**, 998–1009.

23 Y. H. Li, J. W. Yu, J. Y. Xi, W. B. Yu, J. C. Liu, Q. Wang, L. J. Song, L. Feng, Y. P. Yan, G. X. Zhang, B. G. Xiao and C. Ma, Fasudil Enhances Therapeutic Efficacy of Neural Stem Cells in the Mouse Model of MPTP-Induced Parkinson's Disease, *Mol. Neurobiol.*, 2019, **54**, 5400–5413.

24 C. S. Piao, A. L. Holloway, M. S. Hong-Routson and M. S. Wainwright, Depression following traumatic brain injury in mice is associated with down-regulation of hippocampal astrocyte glutamate transporters by thrombin, *J. Cerebr. Blood. Flow. Metab.*, 2019, **39**, 58–73.

25 M. Biro, M. A. Munoz and W. Weninger, Targeting Rho-GTPases in immune cell migration and inflammation, *Br. J. Pharmacol.*, 2014, **171**, 5491–5506.

26 S. Chen, M. Luo, Y. Zhao, Y. Zhang, M. He, W. Cai and A. Liu, Fasudil Stimulates Neurite Outgrowth and Promotes Differentiation in C17.2 Neural Stem Cells by Modulating Notch Sigalling but Autophagy, *Cell. Physiol. Biochem.*, 2015, **36**, 531–541.

27 J. Yu, X. Luan, S. Lan, B. Yan and A. Maier, Fasudil, a Rho-Associated Protein Kinase Inhibitor, Attenuates Traumatic Retinal Nerve Injury in Rabbits, *J. Mol. Neurosci.*, 2016, **58**, 74–82.

28 C. Radoi, T. Garcia, C. Brugniart, A. Ducasse and C. Arndt, Intravitreal triamcinolone injections in non-arteritic anterior ischemic optic neuropathy, *Graefe's Arch. Clin. Exp. Ophthalmol.*, 2014, **252**, 339–345.

29 T. Pannicke, I. Iandiev, A. Wurm, O. Uckermann, H. F. Vom and A. Reichenbach, Diabetes alters osmotic swelling characteristics and membrane conductance of glial cells in rat retina, *Diabetes*, 2006, **55**, 633–639.

30 X. Zhang, S. Bao, D. Lai, R. W. Rapkins and M. C. Gillies, Intravitreal triamcinolone acetonide inhibits breakdown of the bloodretinal barrier through differential regulation of VEGF-A and its receptors in early diabetic rat retinas, *Diabetes*, 2008, **57**, 1026–1033.

31 D. Wang, M. Luo, B. Huang, W. Gao, Y. Jiang, Q. Li, K. Nan and S. Lin, Localized co-delivery of CNTF and FK 506 using a thermosensitive hydrogel for retina ganglion cells protection after traumatic optic nerve injury, *Drug Delivery*, 2020, **27**, 556–564.

32 W. Ong, C. Pinese and S. Y. Chew, Scaffold-mediated sequential drug/gene delivery to promote nerve regeneration and remyelination following traumatic nerve injuries, *Adv. Drug Delivery Rev.*, 2019, **149–150**, 19–48.

33 K. Abhinav, Y. Acosta, W. H. Wang, L. R Bonilla, M. Koutourousiou, E. Wang, C. Synderman, P. Gardner and J. C. Fernandez-Miranda, Endoscopic endonasal approach to the optic canal: anatomic considerations and surgical relevance, *Operative Neurosurgery*, 2015, **11**, 431–446.

34 S. Kehoe, X. F. Zhang and D. Boyd, FDA approved guidance conduits and wraps for peripheral nerve injury: A review of materials and efficacy, *Injury*, 2012, **43**, 553–572.

35 A. Di Somma, L. M. Cavallo, M. de Notaris, D. Solari, T. E. Topczewski, M. Bernal-sprekelsen, J. Enseñat, A. Prats-Galino and P. Cappabianca, Endoscopic endonasal medial-to-lateral and transorbital lateral-to medial optic nerve decompression: an anatomical study with surgical implications, *J. Neurosurg.*, 2017, **127**, 199–208.

36 E. Binstock, A. Bentolila, N. Kumar, H. Harel and A. J. Domb, Preparation, characterization, and sterilization of hydrogel sponges for iontophoretic drug-delivery use, *Polym. Adv. Technol.*, 2007, **18**, 720–730.

37 P. M. D'Onofrio, A. P. Shabanzadeh, B. K. Choi, M. Bähr and P. D. Koeberle, MMP inhibition preserves integrin ligation and FAK activation to induce survival and regeneration in RGCs following optic nerve damage, *Invest. Ophthalmol. Visual Sci.*, 2019, **60**, 634–649.

38 E. Zhang, C. Zhu, J. Yang, H. Sun, X. Zhang, S. Li, Y. Wang, L. Sun and F. Yao, Electrospun PDLLA/PLGA composite membranes for potential application in guided tissue regeneration, *Mater. Sci. Eng., C*, 2016, **58**, 278–285.

39 J. H. Brown, P. Das, M. D. DiVito, D. Ivancic, L. P. Tan and J. A. Wertherim, Nanofibrous PLGA electrospun scaffolds modified with type i collagen influence hepatocyte function and support viability *in vitro*, *Acta Biomater.*, 2018, **73**, 217–227.

40 J. M. Kwong, A. Quan, H. Kyung, N. Piri and J. Caprioli, Quantitative analysis of retinal ganglion cell survival with Rbpms immunolabeling in animal models of optic neruopathies, *Invest. Ophthalmol. Visual Sci.*, 2011, **52**, 9694–9702.

41 L. Benowitz and A. Routtenberg, GAP-43: an intrinsic determinant of neuronal development and plasticity, *Trends Neurosci.*, 1997, **20**, 84–91.

42 C. Dinocourt, S. E. Gallagher and S. M. Thompson, Injury-induced axonal sprouting in the hippocampus is initiated by activation of trkB receptors, *Eur. J. Neurosci.*, 2006, **24**, 1857–1866.

43 D. Giuri, M. Barbalinardo, G. Sotgiu, R. Zamboni, M. Nocchetti, A. Donnadio, F. Corticelli, F. Valle, C. G. M. Gennari, F. Selmin, T. Posati and A. Aluigi, Nano-hybrid electrospun non-woven mats made of wool keratin

and hydrotalcites as potential bio-active wound dressings, *Nanoscale*, 2019, **11**, 6422–6430.

44 M. Hajikhani, Z. Emam-Djomeh and G. Askari, Fabrication and characterization of mucoadhesive bioplastic patch *via* coaxial polylactic acid (PLA) based electrospun nanofibers with antimicrobial and wound healing application, *Int. J. Biol. Macromol.*, 2021, **172**, 143–153.

45 F. Chen, P. Le, G. M. Fernandes-Cunha, S. C. Heilshorn and D. Myung, mBio-orthogonally crosslinked hyaluronate-collagen hydrogel for suture-free corneal defect repair, *Biomaterials*, 2020, **255**, 120176–120185.

46 S. S. Hayreh and M. B. Zimmerman, Non-arteritic anterior ischemic optic neuropathy: role of systemic corticosteroid therapy, *Graefe's Arch. Clin. Exp. Ophthalmol.*, 2008, **246**, 1029–1046.

47 K. Yamashita, Y. Kotani and Y. Nakajima, Fasudil, a Rho kinase(ROCK) inhibitor, protects against ischemic neuronal damage *in vitro* and *in vivo* by acting directly on neurons, *Brain Res.*, 2007, **1154**, 215–224.

48 J. H. Wu, J. Z. Li, H. K. Hu, P. Liu, Y. X. Fang and D. F. Wu, Rho-kinase inhibitor, fasudil, prevents neuronal apoptosis *via* Akt activation and PTEN inactivation in ischemic penumbra of rat brain, *Cell. Mol. Neurobiol.*, 2012, **32**, 1187–1197.

49 C. K. Leung, R. N. Weinreb, Z. W. Li, S. Liu, J. D. Lindsey, N. Choi, L. Liu, C. Y. Cheung, C. Ye, K. Qiu, L. J. Chen, W. H. Yung, J. G. Crowston, M. Pu, K. F. So, C. P. Pang and D. S. C. Lam, Long-term *in vivo* imaging and measurement of dendritic shrinkage of retinal ganglion cells, *Invest. Ophthalmol. Visual Sci.*, 2011, **52**, 1539–1547.